



Measurement of the $(\text{Gd},\text{La})_2\text{O}_2\text{S}:\text{Tb}$ phosphor efficiency for x-ray imaging applications

D. Cavouras^{a,*}, I. Kandarakis^a, C.D. Nomicos^b, A. Bakas^b, G.S. Panayiotakis^c

^aDepartment of Medical Instrumentation Technology, Technological Educational Institution of Athens, Agiou Spyridonos Street, Aigaleo, 122 10 Athens, Greece

^bDepartment of Electronics, Technological Educational Institution of Athens, Agiou Spyridonos Street, Aigaleo, 122 10 Athens, Greece

^cDepartment of Radiology, Technological Educational Institution of Athens, Agiou Spyridonos Street, Aigaleo, 122 10 Athens, Greece

Received 10 October 1998; received in revised form 27 July 1999; accepted 28 July 1999

Abstract

$(\text{Gd},\text{La})_2\text{O}_2\text{S}:\text{Tb}$ phosphor performance was tested under x-ray excitation for medical imaging applications with tube voltages from 70 to 180 kVp and phosphor coating weights from 20 to 240 mg/cm². The emission spectrum of $(\text{Gd},\text{La})_2\text{O}_2\text{S}:\text{Tb}$ was also measured and it was centered at 549 nm. $(\text{Gd},\text{La})_2\text{O}_2\text{S}:\text{Tb}$ was found efficient in a wide range of x-ray tube voltages and adequately compatible with photocathodes, photodiodes, and orthochromatic films currently used in x-ray medical imaging. © 2000 Elsevier Science Ltd. All rights reserved.

1. Introduction

Phosphor materials are employed as radiation to light converters in detectors of x-ray or gamma ray medical imaging systems (Arnold, 1979; Haque and Stanley, 1981; Zweig and Zweig, 1983; Yaffe and Rowlands, 1997). The light emitted by phosphors is usually captured by optical detectors (films, photocathodes or photodiodes) incorporated in the radiation detector system. $\text{Gd}_2\text{O}_2\text{S}:\text{Tb}$ and $\text{La}_2\text{O}_2\text{S}:\text{Tb}$ have been previously shown to be two of the most efficient phosphors (Giakoumakis et al., 1989; Kandarakis et al., 1996). $\text{Gd}_2\text{O}_2\text{S}:\text{Tb}$ is efficient at medium to high diagnostic x-ray energies while $\text{La}_2\text{O}_2\text{S}:\text{Tb}$ is more efficient at lower energies. $\text{Gd}_2\text{O}_2\text{S}:\text{Tb}$ is widely used in radiographic intensifying screens and in detectors of digital

radiographic units while $\text{La}_2\text{O}_2\text{S}:\text{Tb}$ is incorporated in intensifying screens of some radiographic cassettes (Arnold, 1979).

In the present study the luminescent properties of a phosphor mixture consisting of 50% $\text{Gd}_2\text{O}_2\text{S}:\text{Tb}$ and 50% $\text{La}_2\text{O}_2\text{S}:\text{Tb}$ were determined, in order to investigate if this mixture is adequately efficient in a wider range of x-ray energies than the energy range of each phosphor used alone. The luminescence evaluation of the mixture, denoted as $(\text{Gd},\text{La})_2\text{O}_2\text{S}:\text{Tb}$, was accomplished by determining the following parameters:

1. The absolute efficiency (**AE**) of the phosphor, which is defined as the ratio of the light energy flux emitted by an irradiated phosphor over the incident x-ray or gamma ray exposure rate (Ludwig, 1971; Cavouras et al., 1996; Kandarakis et al., 1996, 1997). AE is very important if the phosphor performance is evaluated in relation to the patient radiation dose burden.
2. The effective efficiency (**EE**), which is the absolute efficiency with respect to the spectral compatibility

* Corresponding author. Tel./fax: +301-9594-558 (home); fax: +301-5910-975 (work).

E-mail address: cavouras@medisp.bme.teiath.gr (D. Cavouras).

between the phosphor's emission spectrum and the spectral sensitivity of the optical detector. EE is very useful for determining the optimum phosphor-optical detector combination (Cavouras et al., 1998). Obviously, EE is a function of the fraction of the primary x-ray beam transmitted through the patient's body. For a given level of patient exposure, a high EE phosphor-optical detector combination produces images of higher brightness.

AE and EE were evaluated for a wide range of phosphor coating weights using x-rays produced by x-ray tube high voltages ranging from 50 to 200 kVp.

2. Materials and methods

2.1. Definitions

2.1.1. The absolute efficiency

The absolute efficiency η of a phosphor is given by the relation:

$$\eta(E_0, w) = \frac{\Psi_\lambda(E_0, \lambda, w)}{\dot{X}(E_0)} \quad (1)$$

where Ψ_λ is the emitted light energy flux (energy of light per unit of area and time), \dot{X} is the incident exposure rate that excites the phosphor to luminescence, E_0 denotes the maximum x-ray energy determined by the tube voltage, w is the coating weight of the phosphor and λ is the wavelength of the emitted light.

AE depends on the following physical properties:

1. The x-ray absorption efficiency, which is determined by the x-ray absorption coefficient (μ) and the coating weight (w) of the phosphor.
2. The intrinsic x-ray to light conversion efficiency (η_c), which expresses the fraction of absorbed x-ray energy that is converted into light. η_c depends on the fundamental energy band gap of the material, the site symmetry and other intrinsic properties of the phosphor.
3. The light transmission efficiency (g), which expresses the fraction of light that is transmitted through the phosphor and is emitted by the phosphor surface. g depends on the light attenuation properties of the material which are functions of light wavelength λ .

2.1.2. The effective efficiency

The effective efficiency (η_{eff}) has been defined (Cavouras et al., 1998) by the formula:

$$\eta_{\text{eff}}(E_0, w) = \eta(E_0, w) \left[\frac{\int_{\lambda} \varepsilon_p(\lambda) S_{\text{OD}}(\lambda) d\lambda}{\int_{\lambda} S_{\text{OD}}(\lambda) d\lambda} \right] \quad (2)$$

where $\varepsilon_p(\lambda)$ is the phosphor's emission spectrum and $S_{\text{OD}}(\lambda)$ is the spectral sensitivity distribution of the optical detector used with the phosphor. The factor within brackets expresses the spectral compatibility of the phosphor's spectrum with respect to the optical detector (Cavouras et al., 1996, 1998).

2.2. Measurements and calculations

To determine AE and EE the following measurements were performed:

1. The light energy flux, Ψ_λ in equation (1) was measured using an EMI 9558 QB photomultiplier equipped with an extended S-20 photocathode and coupled to a Carry 401 electrometer. Measurements were performed following two modes of light observation: (a) Transmission mode or front screen configuration set-up, where the light emitted was measured from the non-irradiated phosphor surface; (b) Reflection mode or back screen configuration set-up, where the light emission from the x-rayed phosphor surface was determined (Cavouras et al., 1996; Kandarakis et al., 1998). Transmission mode simulates practically all types of medical imaging detector configurations: CT, gamma camera, digital radiography detectors, image intensifiers and front screen of radiographic cassettes. Reflection mode simulates conventional mammography cassettes and back screens of radiography cassettes. To accurately determine Ψ_λ , the experimental data were corrected dividing by: (a) the spectral compatibility (see factor in brackets in relation (6)) between the (Gd,La)₂O₂S:Tb phosphor light and the spectral sensitivity of the S-20 photocathode of the measuring instrument; and (b) the geometric light collection efficiency of the phosphor-photocathode configuration. This efficiency depends on the angular distribution of emitted light, which was determined as previously described (Giakoumakis and Miliotis, 1985), and on the distance between the phosphor layer and the photomultiplier.
2. The exposure rate, \dot{X} in relation (1) was measured by a PTW dosimeter (ionization chamber type No. 23333). X-ray exposures were performed on a Siemens Stabilipan x-ray unit with high voltages from 70 to 180 kVp.
3. The phosphor's emission spectrum, $\varepsilon_p(\lambda)$ in Eq. (2), was measured by an Oriel 7240 grating monochromator. Spectral sensitivity curves, $S_{\text{OD}}(\lambda)$ in relation (2), were obtained from manufacturer's data.

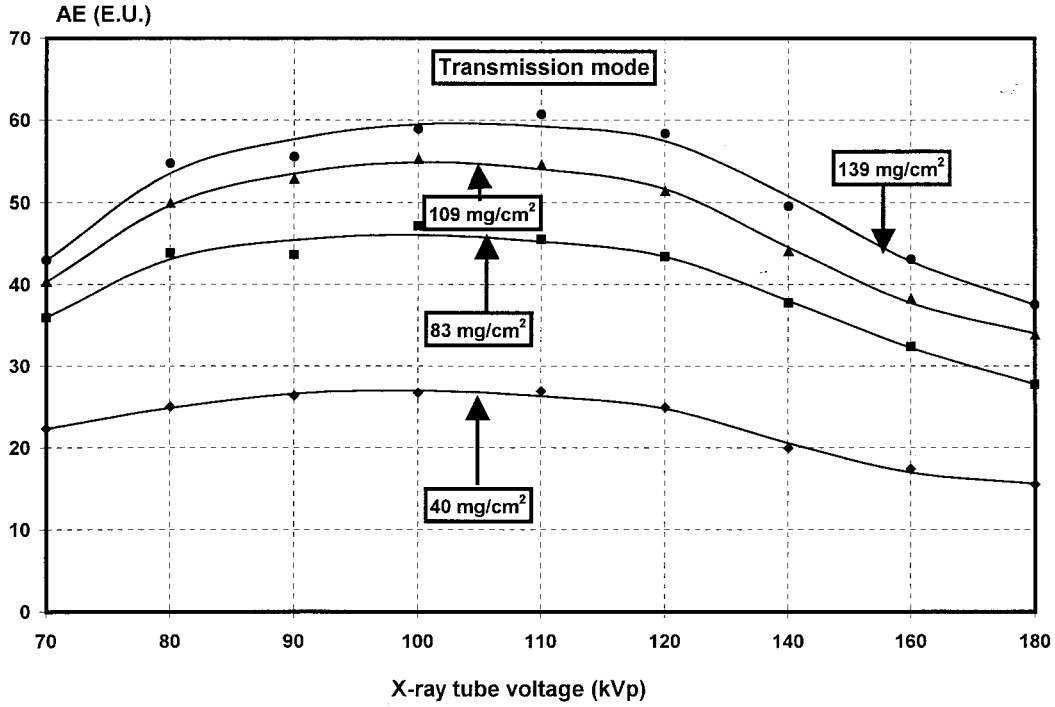


Fig. 1. Variation of $(\text{Gd,La})_2\text{O}_2\text{S:Tb}$ absolute efficiency with x-ray tube voltage, measured in transmission mode, for four screens of 40, 83, 109, and 139 mg/cm^2 coating weight. (1 Efficiency Unit, 1 E.U. = $1 \mu\text{W m}^{-2}/\text{mR s}^{-1}$ or $3.875 \text{ J/C.kg}^{-1}.\text{m}^2$ in S.I. units). Points represent experimental values and solid lines represent theoretical curves.

Phosphor layers (screens) were prepared by sedimentation of the phosphor powder consisting of 50% $\text{Gd}_2\text{O}_2\text{S:Tb}$ and 50% $\text{La}_2\text{O}_2\text{S:Tb}$. Sedimentation was performed on fused silica substrates using Na_2SiO_3 as binding material between the phosphor powder grains (mean size: $7 \mu\text{m}$). The coating weight of the various phosphor layers prepared ranged from 20 to 240 mg/cm^2 , which correspond to the coating thicknesses of phosphor screens, or other detector types, used in medical imaging.

2.3. Theoretical interpretation

Absolute efficiency was also theoretically calculated as a function of parameters related to x-ray absorption, x-ray to light conversion, and light attenuation properties of the phosphor material [see appendix] by the following general expression:

$$\eta(E_0, w) = \eta_C f(\sigma, \beta, \rho, \mu) \quad (3)$$

where σ , β are optical parameters given as functions of light absorption (a) and light scattering (s) coefficients of the phosphor by the following relations:

$$\sigma = \sqrt{a(a+2s)} \quad \text{and} \quad \beta = \sqrt{a/(a+2s)}$$

ρ in Eq. (3) is a parameter related to light reflectivities (r) at the phosphor layer surfaces as follows:

$$\rho = \frac{1-r}{1+r}$$

Parameter β has been also expressed (Ludwig, 1971) as a function of the light reflectivity (r_∞) at a very thick phosphor layer (w_∞) through which light cannot be transmitted:

$$\beta = \frac{1-r_\infty}{1+r_\infty}$$

μ is the x-ray absorption coefficient of the phosphor.

Relation (3) was used to fit experimental absolute efficiency data. Parameters β and ρ were measured by reflectivity measurements as described by Ludwig (Ludwig, 1971). Coefficient μ was calculated using data on Gd, La, O, S from Storm and Israel (Storm and Israel, 1967). Intrinsic efficiency η_C was set equal to 0.19, since in previous studies (Kandarakis et al., 1996, 1997) η_C was found equal to 0.18 and 0.20 for $\text{La}_2\text{O}_2\text{S:Tb}$ and $\text{Gd}_2\text{O}_2\text{S:Tb}$ respectively. Thus, to obtain best fitting between experimental and calculated results, only parameter σ was allowed to vary.

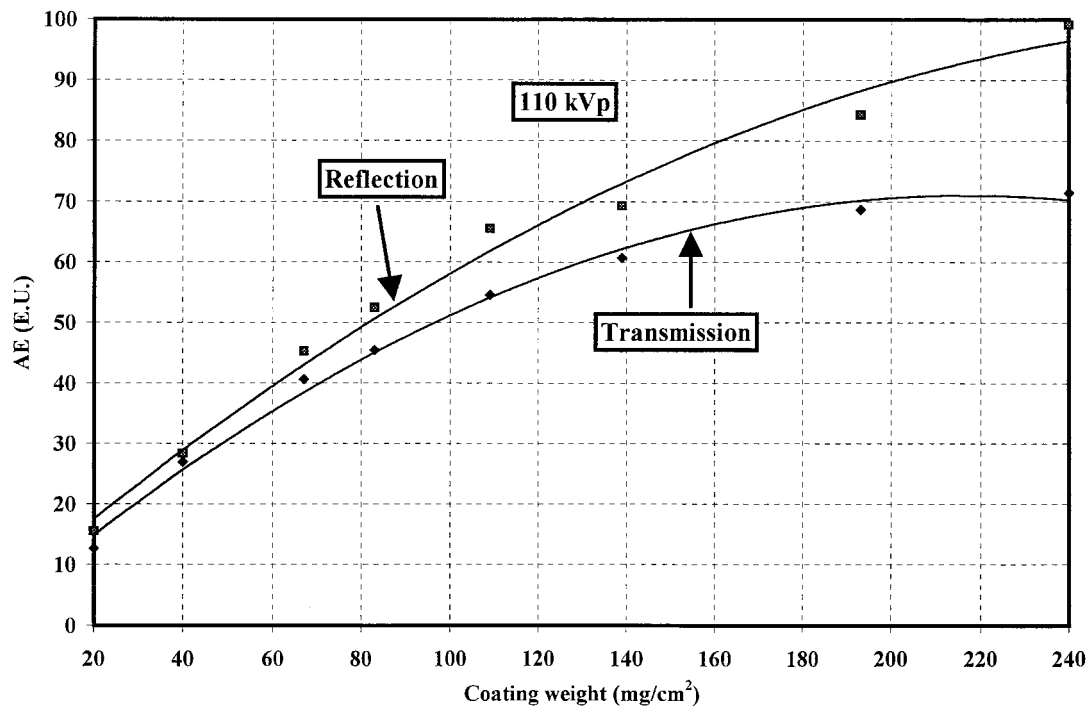


Fig. 2. Variation of $(\text{Gd,La})_2\text{O}_2\text{S:Tb}$ absolute efficiency with coating weight for reflection and transmission mode, measured at 110 kVp x-ray tube voltage. (1 Efficiency Unit, 1 E.U. = $1 \mu\text{W m}^{-2}/\text{mR s}^{-1}$ or $3.875 \text{ J/C.kg}^{-1} \cdot \text{m}^2$ in S.I. units). Points represent experimental values and solid lines represent theoretical curves.

3. Results and discussion

The variation of $(\text{Gd,La})_2\text{O}_2\text{S:Tb}$ absolute efficiency with x-ray tube's high voltage, measured in transmission mode is plotted in Fig. 1. Points represent experimental values while solid lines represent theoretical curves. The latter were obtained by fitting relations (3), (A8) and (A9) of the appendix, to experimental data, using the Levenberg–Marquard method (Press et al., 1990). Best fitting was obtained for $\sigma = 30 \text{ cm}^2/\text{g}$. Only four coating weights are depicted in Fig. 1, since all curves had similar shape. In the tube voltage range between 80 and 120 kVp, AE varies slowly maintaining high values. At low coating weight (40 mg/cm^2), AE exhibits an almost flat response within the 80–120 kVp voltage range. These results are interesting for medical imaging since the aforementioned voltage range is often employed in radiography, fluoroscopy and in computed tomography. This response was expected and may be easily explained considering the different behaviour of the two phosphors constituting the mixture. Previous studies (Giakoumakis et al., 1989; Kandarakis et al., 1996) have shown that peak absolute efficiency is expected to appear at around 80 kVp for $\text{La}_2\text{O}_2\text{S:Tb}$ and at 110 kVp for $\text{Gd}_2\text{O}_2\text{S:Tb}$. These data are compatible with results shown in Fig. 1,

where high AE values were observed in a rather wide kVp range. For voltages higher than 120 kVp, absolute efficiency shows a rather rapid decrease. This is principally due to the low x-ray absorption at high x-ray energies which in turn reduces the efficiency of light production and hence AE. The latter was also found to decrease at low voltages. This happens because low energy x-ray quanta are absorbed very close to the phosphor's irradiated surface, causing the optical quanta to travel a long distance to escape from the other surface of the phosphor. Thus, light is seriously attenuated before emission.

In Fig. 2 the variation of AE with coating weight is plotted for both reflection and transmission mode measurements, performed at 110 kVp. As it is observed the values of absolute efficiency in reflection mode are higher than those in transmission mode, for equal coating weight. This difference is explained by considering that most of the incident x-ray quanta are absorbed not very deep from the irradiated phosphor surface. This may be quantitatively estimated by calculating the x-ray absorption efficiency of the phosphor as a function of x-ray penetration depth (see Appendix A2). Results of the calculations, concerning the 110 kVp beam, were obtained using Eq. (A13) of the Appendix and are shown in Fig. 3. As it is observed,

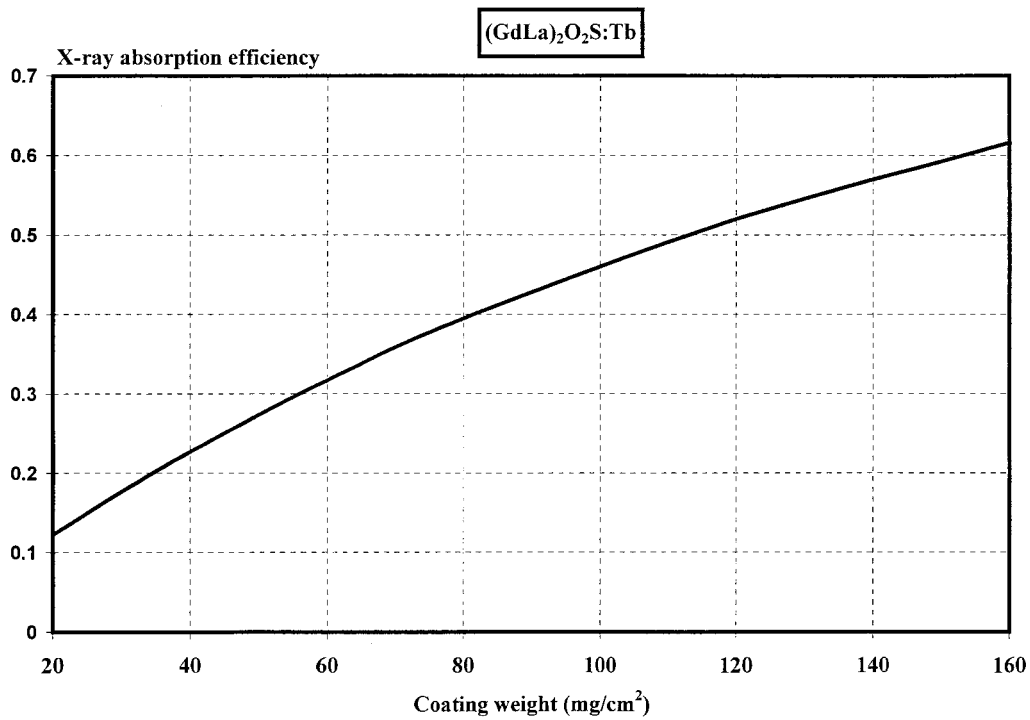


Fig. 3. Variation of x-ray absorption efficiency with x-ray penetration depth. Curve has been generated using Eq. (A13) of Appendix A.

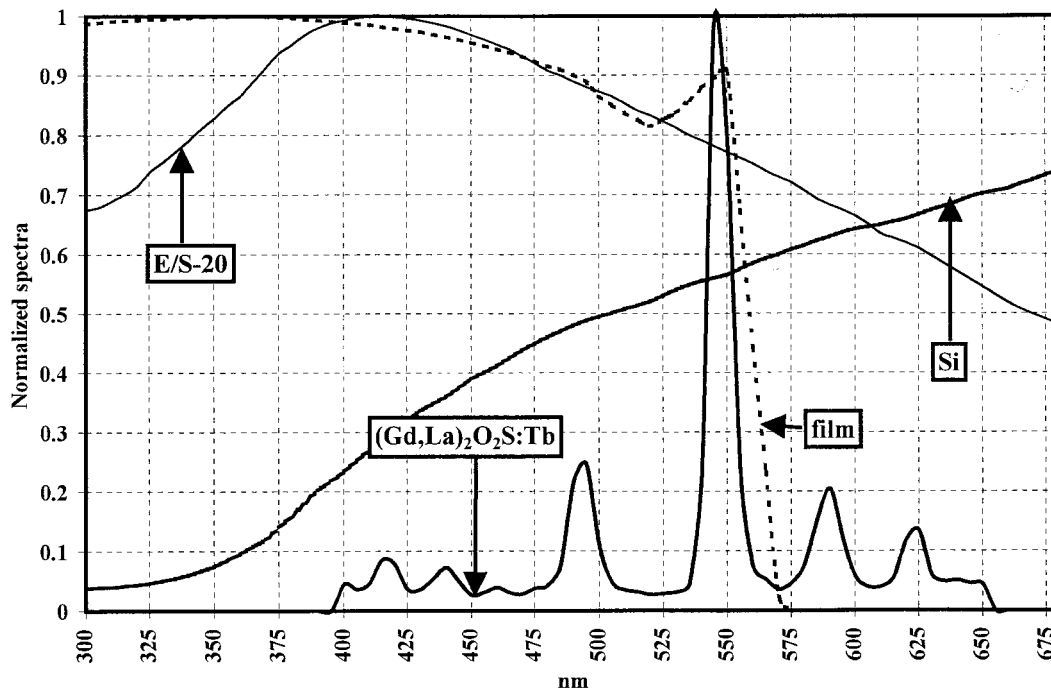


Fig. 4. Normalized spectral response of the $(\text{Gd,La})_2\text{O}_2\text{S:Tb}$ phosphor against normalized spectral sensitivities of various optical detectors.

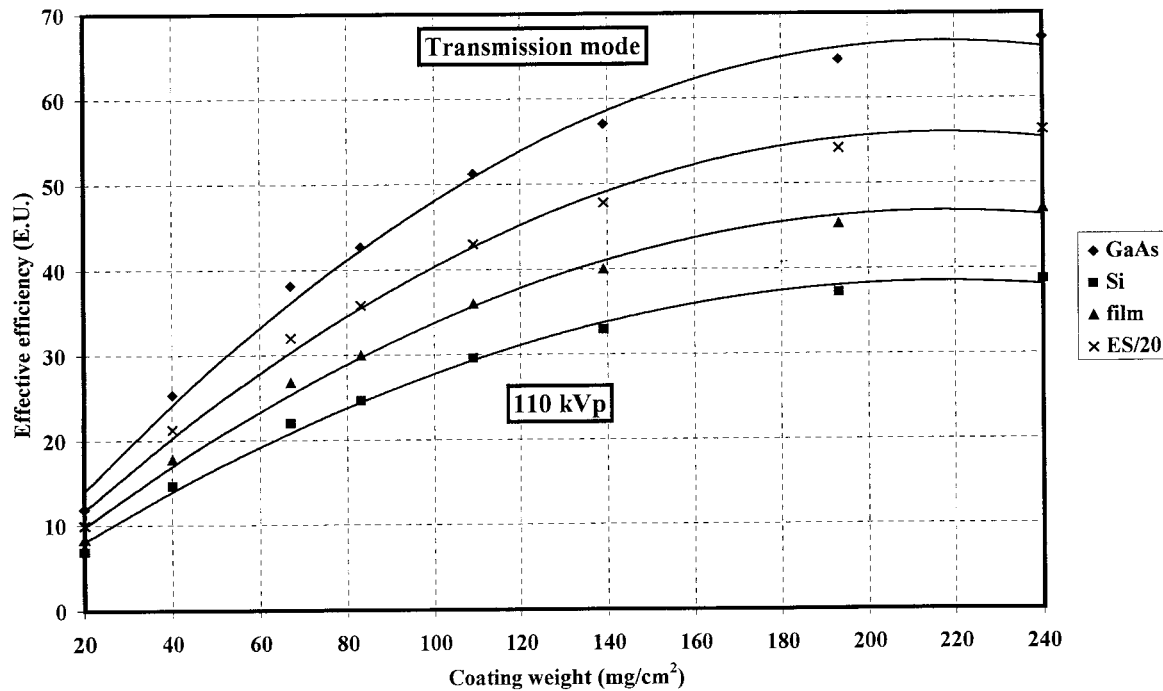


Fig. 5. Variation of the effective efficiency of $(\text{Gd,Lu})_2\text{O}_2\text{S:Tb}$ with coating weight, determined in transmission mode and with respect to various optical detectors. (1 Efficiency Unit, 1 E.U. = $1 \mu\text{W m}^{-2}/\text{mR s}^{-1}$ or $3.875 \text{ J/C.kg}^{-1}.\text{m}^2$ in S.I. units).

for the 100 mg/cm^2 layer, 60% of the incident x-ray quanta are absorbed within the 50 mg/cm^2 depth. Hence optical quanta have to penetrate shorter distances to escape from the irradiated surface than from the non irradiated one. Consequently, the intensity of light suffers lower attenuation in reflection mode. The divergence between the two curves, as shown in Fig. 2, augments with increasing coating weight. AE in reflection mode increases continuously while in transmission mode the slope of the curve is lower and it seems to attain a plateau at high coating weights. This phenomenon results from the significantly longer trajectories that light travels in transmission mode than in reflection mode when the phosphor is thick. Long photon trajectories cause an increase in: (1) light attenuation due to both light absorption and scattering effects and in (2) light spread at the phosphor output. On the other hand, in reflection mode the photon trajectories increase slowly with phosphor thickness and the plateau should be expected to appear at higher coating weights.

Fig. 4 shows the measured emission spectrum of $(\text{Gd,Lu})_2\text{O}_2\text{S:Tb}$ normalized to unity. The spectrum contains four main lines centered at 493, 549, 589 and 623 nm. The highest peak is the one lying in the green region (549 nm) of the visible spectrum. The $(\text{Gd,Lu})_2\text{O}_2\text{S:Tb}$ spectrum is very similar to the spectra

of $\text{Gd}_2\text{O}_2\text{S:Tb}$ and $\text{La}_2\text{O}_2\text{S:Tb}$. However, the highest peak, as well as the other lower peaks, are very slightly displaced towards higher wavelengths as compared to the corresponding spectrum of $\text{Gd}_2\text{O}_2\text{S:Tb}$ (highest peak at 545 nm), measured under the same conditions. In the same figure the spectral sensitivity curves of various optical detectors used in diagnostic imaging are plotted. The principal uses of these detectors are: (1) the films Agfa Curix Ortho GS, Kodak X-omatic GR, and Fuji UM-MH are orthochromatic films exhibiting high sensitivity to the green light and they are often used in conventional radiographic cassettes. Only one film is shown since the sensitivity curves of the three films did not differ significantly; (2) the E/S-20 photo-

Table 1
Spectral compatibility of $(\text{Gd,Lu})_2\text{O}_2\text{S:Tb}$, $\text{Gd}_2\text{O}_2\text{S:Tb}$, and CsI:Na phosphors with various optical detectors

Optical detectors	Phosphors		
	$(\text{Gd,Lu})_2\text{O}_2\text{S:Tb}$	$\text{Gd}_2\text{O}_2\text{S:Tb}$	CsI:Na
GaAs	0.939	0.938	0.917
E/S 20	0.788	0.784	0.934
Si	0.542	0.533	0.309
Orthochromatic film	0.659	0.701	0.943

cathode used in image intensifiers employed either in fluoroscopy or in some types of digital imaging detectors (Yaffe and Rowlands, 1997). E/S-20 is also used in photomultipliers of nuclear medicine detectors; (3) the Silicon (Si) photodiode used in CCD arrays of digital radiography and computed tomography detectors.

The EE of (Gd,La)₂O₂S:Tb in transmission mode with respect to optical detectors is plotted in Fig. 5 as a function of the coating weight. Spectral compatibility data, determined using the term in brackets in Eq. (2), are shown in Table 1. (Gd,La)₂O₂S:Tb is most efficient in combination with the E/S-20 photocathode in diagnostic imaging. It is also adequately efficient with the orthochromatic films.

Data concerning Gd₂O₂S:Tb and CsI:Na phosphors, determined in our laboratory, are also shown in Table 1 for comparison. Gd₂O₂S:Tb is currently used in intensifying screens and in some digital radiography detectors while CsI:Na is used in image intensifiers (Arnold, 1979; Yaffe and Rowlands, 1997). As it can be observed from Table 1, (Gd,La)₂O₂S:Tb showed highest spectral compatibility values with the photocathodes and the orthochromatic film. However, the spectral compatibility of the Gd₂O₂S:Tb-film and the CsI:Na–E/S-20 combinations were found higher than the corresponding (Gd,La)₂O₂S:Tb-film and (Gd,La)₂O₂S:Tb–E/S-20 combinations. On the other hand, (Gd,La)₂O₂S:Tb, when combined with the Si photodiode, provided better spectral matching than the corresponding combinations of the two other phosphors. These data show that although (Gd,La)₂O₂S:Tb is suitable for use with image intensifiers or radiographic cassettes, however, when combined with the photodiodes of digital imaging detectors it provides a better combination than the corresponding combinations of Gd₂O₂S:Tb or CsI:Na. It is also worth noting that (Gd,La)₂O₂S:Tb showed very high compatibility with the GaAs photocathode used in some image intensifiers and photomultipliers for non medical applications

In conclusion, (Gd,La)₂O₂S:Tb is a phosphor material that exhibits high performance in a wide range of x-ray tube voltages, as compared to Gd₂O₂S:Tb and La₂O₂S:Tb, covering the demands of various x-ray examinations.

Acknowledgements

This study is dedicated to the memory of Professor G.E. Giakoumakis, leading member of our team, whose work on phosphor materials has inspired us to continue.

Appendix A

A.1. Calculation of absolute efficiency

Consider a phosphor layer of thickness w_0 sandwiched between two partially reflecting media (substrates) irradiated by x-rays. The fraction of incident x-ray energy flux absorbed in an elementary thin phosphor layer dw at depth w , is given by the relation:

$$d\Psi_X^{\text{ab}}(E, w) = -\mu(E)\Psi_X(E, 0) \exp[-\mu(E)w] dw \quad (\text{A1})$$

where $\mu(E)$ is the x-ray mass absorption coefficient of the phosphor material and $\Psi_X(E, 0)$ is the x-ray energy flux incident on the surface ($w = 0$) of the phosphor layer. The exponential factor $\exp[-\mu(E)w]$ accounts for the attenuation of $\Psi_X(E, 0)$ during its penetration through the phosphor material at depth w before reaching the elementary thin layer dw . The light energy flux ($d\Psi_\lambda$) created within this thin layer is given as:

$$d\Psi_\lambda(w) = \eta_C \mu(E)\Psi_X(E, 0) \exp[-\mu(E)w] dw \quad (\text{A2})$$

where η_C is the intrinsic x-ray to light conversion efficiency of the phosphor material. One half of this light energy flux is directed towards the irradiated phosphor surface (reflection mode) and one half towards the opposite non-irradiated surface (transmission mode). By taking into account the effects of light absorption and scattering, the light energy flux $d\Psi_\lambda^{\text{T}}(E, w)$ created within dw and directed towards the non irradiated phosphor surface and $d\Psi_\lambda^{\text{R}}(E, w)$ created within dw and directed towards the irradiated surface are:

$$d\Psi_\lambda^{\text{T}}(E, w) = -(a + s)\Psi_\lambda^{\text{T}}(E, w) dw + s\Psi_\lambda^{\text{R}}(E, w) dw + \frac{1}{2}\eta_C \mu(E) \exp[-\mu(E)w]\Psi_X(E, 0) dw \quad (\text{A3})$$

$$d\Psi_\lambda^{\text{R}}(E, w) = (a + s)\Psi_\lambda^{\text{R}}(E, w) dw - s\Psi_\lambda^{\text{T}}(E, w) dw - \frac{1}{2}\eta_C \mu(E) \exp[-\mu(E)w]\Psi_X(E, 0) dw \quad (\text{A4})$$

where a is the light absorption coefficient of the phosphor, s is the light scattering coefficient, $\Psi_\lambda^{\text{T}}(E, w)$ is the light energy flux at depth w , traveling towards the non-irradiated side and $\Psi_\lambda^{\text{R}}(E, w)$ the light energy flux towards the irradiated one. Superscripts T and R denote transmission (direction towards the non-irradiated surface) and reflection (direction towards the irradiated surface) respectively. Functions Ψ_λ^{T} and Ψ_λ^{R} may be obtained as solutions of the two differential Eqs. (A3) and (A4). The absolute efficiency in transmission (η_{T}) and in reflection (η_{R}) modes of the phosphor layer of coating weight w_0 may then be defined as:

$$\eta_T(E, w_0) = \frac{t_T}{[\dot{X}/\Psi_X]} \frac{\Psi_\lambda^T(E, w_0)}{\Psi_X(E, 0)} \quad (\text{A5})$$

$$\eta_R(E, w_0) = \frac{t_R}{[\dot{X}/\Psi_X]} \frac{\Psi_\lambda^T(E, 0)}{\Psi_X(E, 0)} \quad (\text{A6})$$

where, t_T and t_R are the light transmissivities of the back and front substrates of the phosphor layer. $[\dot{X}/\Psi_X]$ is a conversion coefficient accounting for the conversion of the x-ray energy flux Ψ_X into exposure rate \dot{X} . This conversion is necessary in order to simulate our experimental conditions where \dot{X} , and not Ψ_X , was measured. This conversion coefficient is given by the relation (Hendee, 1970; Greening, 1985):

$$\frac{\dot{X}}{\Psi_X} = \left[\frac{\mu_{\text{en}}}{\rho} \right]_{\text{air}} \frac{e}{W_{\text{air}}} \quad (\text{A7})$$

where W_{air} is the average energy required to produce an ion pair in air, $[\mu_{\text{en}}/\rho]_{\text{air}}$ is the mass x-ray energy absorption coefficient in air and e is the electron charge. Taking into account the expressions for Ψ_λ after solution of Eqs. (A3) and (A4), the absolute efficiency in transmission and reflection modes can be finally written as (Ludwig, 1971; Cavouras et al., 1996):

$$\eta_T(E, w_0) = \frac{\eta_c t_T \mu(E) (1 + \rho_0) e^{-\mu(E)w_0}}{\left[\frac{\dot{X}}{\Psi_X} \right] \times 2(\mu(E)^2 - \sigma^2)} \times \frac{(\mu(E) - \sigma)(1 - \beta) e^{-\sigma w_0} + 2(\sigma + \mu(E)\beta) e^{\mu(E)w_0} - (\mu(E) + \sigma)(1 + \beta) e^{\sigma w_0}}{(1 + \beta)(\rho_0 + \beta) e^{\sigma w_0} - (1 - \beta)(\rho_0 - \beta) e^{-\sigma w_0}} \quad (\text{A8})$$

for transmission mode and

$$\eta_R(E, w_0) = \frac{\eta_c t_R \mu(E) e^{-\mu(E)w_0}}{\left[\frac{\dot{X}}{\Psi_X} \right] \times (\mu(E)^2 - \sigma^2)} \times \frac{(\mu(E) - \sigma)(\rho_0 + \beta) e^{-\sigma w_0} + 2(\sigma \rho_0 - \mu(E)\beta) e^{-\mu(E)w_0} - (\mu(E) + \sigma)(\rho_0 - \beta) e^{-\sigma w_0}}{(1 + \beta)(\rho_0 + \beta) e^{\sigma w_0} - (1 - \beta)(\rho_0 - \beta) e^{-\sigma w_0}} \quad (\text{A9})$$

for reflection mode where: $\rho_0 = \frac{1-r}{1+r}$, where r is the reflectivity of the screen substrate. Here, we have considered only one substrate, since this was the case of our experiments. Hence, t_R in (A9) was considered equal to 1.

σ , β : coefficients directly related to the absorption (a) and scattering (s) coefficients of optical photons within the screen, by:

$$\sigma = [a(a + 2s)]^{1/2} \text{ and } \beta = [a/(a + 2s)]^{1/2}$$

Furthermore, to simulate experimental conditions, where polyenergetic x-ray beams were used, absolute

efficiency η was averaged over the x-ray energy spectrum $[d\Psi_X(E)/dE]_S$

$$\eta(E_0, w_0) = \frac{\int_0^{E_0} \left[\frac{d\Psi_X(E)}{dE} \right]_S \eta(E, w_0) dE}{\int_0^{E_0} \left[\frac{d\Psi_X(E)}{dE} \right]_S dE} \quad (\text{A10})$$

where E_0 is the maximum energy of the spectrum and $[d\Psi_X(E)/dE]_S$ denotes the x-ray spectral density distribution (energy flux per energy interval) (Tucker et al., 1991).

A.2. Calculation of x-ray quantum absorption efficiency

To calculate the fraction of x-ray quanta absorbed at a depth w within a phosphor layer, relation (A1) has to be integrated over w and then to be divided by the incident x-ray quantum fluence:

$$\eta_X^{\text{ab}}(E, w) = \frac{\Psi_X^{\text{ab}}(E, w)}{\Psi_X(E, 0)} = \frac{1}{\Psi_X(E, 0)} \int_0^w \mu(E) \Psi_X(E, 0) \exp[-\mu(E)w] dw \quad (\text{A12})$$

For polyenergetic x-ray beams both numerator and denominator of (A12) must be integrated over the energy range:

$$\eta_X^{\text{ab}}(E_0, w) = \frac{\int_0^{E_0} \mu(E) \left[\frac{d\Psi_X(E)}{dE} \right]_S \int_0^w \exp[-\mu(E)w] dw dE}{\int_0^{E_0} \left[\frac{d\Psi_X(E)}{dE} \right]_S dE} \quad (\text{A13})$$

A.3. Calculation of x-ray spectral density distribution

The incident x-ray energy flux $\Psi_x(E)$ may be expressed as:

$$\Psi_x(E) = N_x(E)E \quad (\text{A14})$$

where, $N_x(E)$ is the x-ray quantum flux (number of incident x-ray quanta per unit of area and time). In the model developed by Tucker (Tucker et al., 1991) for x-ray spectra, the number $N_x(E)$ of x-ray quanta produced by the bremsstrahlung process with energy between E and $E + dE$ is given as follows:

$$\begin{aligned} N_x(E)dE &= [\alpha r_e Z^2 / A] \\ &\times [dE/E] \int_E^{E_0} B \frac{(E_c + m_0 c^2)}{E_c} F(E, E_c, E_0) \\ &\times \left[\frac{1}{\rho_A} \frac{dE_c}{dx} \right]^{-1} dE_c \end{aligned} \quad (\text{A15})$$

where N_x is the x-ray quantum fluence per keV, α is the fine structure constant, r_e is the classical electron radius, Z is the atomic number of the target material (x-ray tube anode) — usually tungsten or molybdenum — A is the mass of the target atoms, E_0 is the kinetic energy of the incident electron, E_c is the penetrating electron energy, m_0 is the rest mass of an electron, c is the light velocity, $(1/\rho_A) [dE_c/dx]$ is the mass stopping power of the target material, $F(E, E_c, E_0)$ is the fraction of x-ray quanta transmitted by the anode given by:

$$F(E, E_c, E_0) = \frac{\exp[-\mu_A(E)(E_0^2 - E_c^2)]}{\rho_A c_{TW} \sin(\vartheta + \varphi)} \quad (\text{A16})$$

where $\mu_A(E)$ and ρ_A are the linear attenuation coefficient and density of the anode material respectively, c_{TW} is the Thomson–Whiddington constant (Tucker et al., 1991), ϑ is the target angle, φ is the angle off the central axis along which an x-ray quantum travels, x is the depth of electron penetration within the target, B is a function of Z and E_0 given by Tucker (Tucker et al., 1991). Most data and functions necessary for $N_x(E)$ calculations were taken from Tucker (Tucker et al., 1991) and from x-ray unit manufacturer's data.

References

Arnold, B.A., 1979. Physical characteristics of screen-film combinations. In: Haus, A.G. (Ed.), *The Physics of Medical Imaging: Recording System, Measurements and*

- Techniques*. American Association of Physicists in Medicine, New York, p. 30.
- Cavouras, D., Kandarakis, I., Panayiotakis, G.S., Evangelou, E.K., Nomicos, C.D., 1996. An evaluation of the $\text{Y}_2\text{O}_3:\text{Eu}^{3+}$ scintillator for application in medical x-ray detectors and image receptors. *Med. Phys.* 23, 1965.
- Cavouras, D., Kandarakis, I., Bakas, A., Triantis, D., Nomicos, C.D., Panayiotakis, G.S., 1998. An experimental method to determine the effective luminescence efficiency of scintillator-photodetector combinations used in x-ray medical imaging systems. *Br. J. Radiol.* 71, 766.
- Giakoumakis, G.E., Miliotis, D.M., 1985. Light angular distribution of fluorescent screens excited by x-rays. *Phys. Med. Biol.* 30, 21.
- Giakoumakis, G.E., Nomicos, C.D., Sandilos, P.X., 1989. Absolute efficiency of $\text{Gd}_2\text{O}_2\text{S}:\text{Tb}$ screens under fluoroscopic conditions. *Phys. Med. Biol.* 34, 673.
- Greening, J.R., 1985. Fundamentals of radiation dosimetry. In: *Medical Physics Handbooks*. Institute of Physics, London.
- Haque, P., Stanley, J.H., 1981. Scintillation crystal-photodiode array detectors. In: Newton, T.H., Potts, D.G. (Eds.), *Radiology of the Skull and Brain: Technical Aspects of Computed Tomography*. CV Mosby Company, St. Louis, MO, p. 4127.
- Hendee, W.R., 1970. *Medical Radiation Physics*. Year Book Medical Publishers, Chicago, p. 145.
- Kandarakis, I., Cavouras, D., Panayiotakis, G.S., Agelis, T., Nomicos, C.D., Giakoumakis, G., 1996. X-ray induced luminescence and spatial resolution of $\text{La}_2\text{O}_2\text{S}:\text{Tb}$ phosphor screens. *Phys. Med. Biol.* 41, 297.
- Kandarakis, I., Cavouras, D., Panayiotakis, G.S., Nomicos, C.D., 1997. Evaluating x-ray detectors for radiographic applications: a comparison of $\text{ZnScdS}:\text{Ag}$ with $\text{Gd}_2\text{O}_2\text{S}:\text{Tb}$ and $\text{Y}_2\text{O}_2\text{S}:\text{Tb}$ screens. *Phys. Med. Biol.* 42, 1351.
- Kandarakis, I., Cavouras, D., Kanellopoulos, E., Nomicos, C.D., Panayiotakis, G.S., 1998. Image quality evaluation of $\text{YVO}_4:\text{Eu}$ phosphor screens for use in x-ray medical imaging detectors. *Radiation Measurements* 29, 481.
- Ludwig, G.W., 1971. X-ray efficiency of powder phosphors. *J. Electrochem. Soc.* 118, 1152.
- Press, W.H., Flannery, B.P., Teukolsky, S.A., Vetterling, W.T., 1990. *Numerical Recipes in C: The Art of Scientific Computing*. Cambridge University Press, Cambridge.
- Storm, E., Israel, H. 1967. Photon cross-sections from 0.001 to 100 MeV for elements 1 through 100 Report LA-3753, Los Alamos Scientific Laboratory, University of California.
- Tucker, D.M., Barnes, G.T., Chakraborty, D.B., 1991. Semi-empirical model for generating tungsten target x-ray spectra. *Med. Phys.* 18, 211–218.
- Yaffe, M.J., Rowlands, J.A., 1997. X-ray detectors for digital radiography. *Phys. Med. Biol.* 42, 1.
- Zweig, G., Zweig, D.A., 1983. Radioluminescent imaging: factors affecting total light output. *Proc. SPIE* 419, 297.